JOURNAL OF GEOPHYSICAL RESEARCH, VOL. 95, NO. C3, PAGES 3049–3060, MARCH 15, 1990

# High-Accuracy, High-Resolution Gravity Profiles From 2 Years of the Geosat Exact Repeat Mission

DAVID T. SANDWELL

*Geological Research Division, Scripps Institution of Oceanography, La Jolla, California*

DAVID C. MCADOO

*National Geodetic Survey, Charting and Geodetic Services, National Ocean Service, NOAA, Rockville, Maryland*

Satellite altimeter data from the first 44 repeat cycles (2 years) of the Geosat Exact Repeat Mission (Geosat ERM) were averaged to improve accuracy, resolution and coverage of the marine gravity field. Individual 17-day repeat cycles (two points per second) were first edited and differentiated resulting in alongtrack vertical deflection (i.e., alongtrack gravity disturbance). To increase the signal to noise ratio, 44 of these cycles were then averaged to form a single, highly accurate vertical deflection profile. The largest contributions to the vertical deflection error is short-wavelength altimeter noise and longer-wavelength oceanographic variability; the combined noise level is typically 6 μrad. Both types of noise are reduced by averaging many repeat cycles. Over most ocean areas the uncertainty of the average profile is less than 1 μrad (0.206 arcsec) which corresponds to 1 mgal of alongtrack gravity disturbance. However, in areas of seasonal ice coverage, its uncertainty can exceed 5 μrad. To assess the resolution of individual and average Geosat gravity profiles, the cross-spectral analysis technique was applied to repeat profiles. Individual Geosat repeat cycles are coherent (> 0.5) for wavelengths greater than about 30 km and become increasingly incoherent at shorter wavelengths. This limit of resolution is governed by the signal-to-noise ratio. Thus when many Geosat repeat profiles are averaged together, the resolution limit typically improves to about 20 km. Except in shallow water areas, further improvements in resolution will be increasingly difficult to achieve because the short-wavelength components are attenuated by upward continuation from the seafloor to the sea surface. These results suggest that the marine gravity field can be completely mapped to an accuracy of 2 mgal and a half-wavelength resolution of 12 km by a 4.5-year satellite altimeter mapping mission.

## INTRODUCTION

Satellite altimetry is becoming a valuable tool for investigating the geology and geophysics of the deep oceans and continental margins. Since the GEOS 3 mission, improvements in altimeter design, orbit accuracy, ionospheric-atmospheric corrections, and tide models have led to substantial improvements in the accuracy and resolution of the geoid profiles acquired by these instruments. One straightforward method of assessing the quality of these data is to compare repeat profiles along the same ground track [Brammer, 1979]. The difference between repeat profiles provides an estimate of the accuracy of the data while the coherence between repeat profiles is used to estimate the resolution capabilities of the data. Analysis of repeating GEOS 3 profiles [*Brammer*, 1979; *Marks and Sailor*, 1986] shows that they can resolve gravity field variations having wavelengths greater than about 75 km. Seasat profiles can resolve wavelengths of about 50 km and greater [*Sailor*, 1982; *Marks and Sailor*, 1986]. The Geosat altimeter, with its lower noise level at short wavelengths [*Sailor and LeSchack*; 1987; *LeSchack and Sailor*, 1988], can resolve features having wavelengths greater than about 30 km [*Born et al.*, 1987; *Sandwell and McAdoo*, 1988].

In this study we have averaged repeat Geosat profiles for the first 2 years of the Exact Repeat Mission (Geosat ERM) [*Cheney et al.*, 1987] in order to improve the coverage, accuracy, and resolution of the data. Because the radial orbit errors for the Geosat ERM are quite large and the repeat profiles contain many irregular gaps, simple averaging of sea surface topography profiles results in short-wavelength errors at the boundaries of data gaps. This averaging problem is effectively eliminated if the profiles are first differentiated before averaging resulting in alongtrack vertical deflection profiles. The differentiation procedure also enhances the short-wavelength gravity signal and noise. To assess the accuracy and resolution of the 2-year average profile on a global basis, the repeat track analysis method is used. We estimate that the 2-year average, vertical deflection profile is accurate to about 1 μrad (0.206 arcsec); features with wavelengths as short as 23 km can be resolved. The implication is that the marine gravity field can be completely mapped to an accuracy of 2 μrad and a resolution of 24-km wavelength by a satellite altimeter placed in a 180-day repeat cycle for 4.5 years. Such a data set would provide an extraordinary view of the ocean basins.



Paper number 89JC03209.
0148-0227/90/89JC-03209$05.00

## DATA PROCESSING

### *Preprocessing*

The first 44 repeat cycles of the Geosat geophysical data record (GDR) altimeter data from November 7, 1986, to November 27, 1988, were used in our analysis. Each 1-per-second GDR includes the following items: 10 sea surface height measurements, the average of the 10 measurements, the standard deviation of the average, environmental corrections, and preprocessing flags [*Cheney et al.*, 1987]. On the basis of the previous experience with Seasat altimeter data [*Marsh and Martin*, 1982] and our experience with Geosat data, the GDRs were edited for the following reasons: standard deviation of 1-per-second average exceeding 0.1 m ; significant wave height greater than 8 m; automatic gain control greater than 34 dB or less than 15 dB, and flagged data over land or ice. This editing eliminated about 16% of the data.

Instead of using the 1-per-second average heights, the 10-per-second observations were averaged into 2-per-second observations. The increased sampling rate retains more of the short-wavelength gravity information and also allows for a more accurate interpolation of the repeat cycles into uniform alongtrack bins. The following corrections (supplied with the GDRs) were then applied to the 2-per-second data: ocean tides (Schwiderski), solid earth tides (Cartwright), ionosphere delay and troposphere delay (both wet and dry components from the Fleet Numerical Oceanography Center (FNOC)). The data were not corrected for the electromagnetic (EM) bias because this correction may introduce an undesirable short-wavelength component. Moreover, the constant of proportionality between significant wave height and radar delay is not well constrained [*Zlotnicki et al.*, 1989]. After the corrections were applied, the data were divided into ascending or descending passes. The passes were further subdivided whenever a time gap exceeded 10 s.

A final step in the preprocessing was to differentiate each profile with respect to time using a first-difference formula. When this alongtrack derivative is divided by the groundtrack speed of the satellite one obtains the alongtrack slope of the sea surface or alongtrack vertical deflection. Vertical deflection is a measure of the horizontal component of the gravity anomaly vector. One microradian of vertical deflection corresponds to 0.98 mgal of alongtrack gravity disturbance.

From a processing standpoint, it is much simpler to average vertical deflection profiles than it is to average sea surface topography profiles. The derivative operation acts a a high-pass filter which suppresses the long-wavelength radial orbit error (and other long-wavelength errors) and enhances the short-wavelength gravity anomalies. After differentiation, 1 to 2-m relative radial orbit errors map into slope errors of less than 0.2 μrad [*Sandwell and Zhang*, 1989], which are smaller than the expected accuracy of the mean profile. Thus vertical deflection profiles can be averaged together on a point by point basis without first performing and tilt and bias correction.

In the case of sea surface topography profiles, the simple averaging does not yield accurate results. The problem is that each profile has a different unknown bias (1–2 m) due to radial orbit error. Large-amplitude steplike artifacts will occur when when one of the profiles has a data gap. Consider averaging a single profile, having a 1-m unknown bias and a data gap, together with 29 other profiles having no data gaps. The average of the 30 profiles will contain an artificial step of 0.033 m at the location of the data gap. Over a distance of 3.4 km, this step maps into a slope artifact of 10 μrad, and thus a gravity map produced with these data would contain a 10-mgal artificial anomaly. As shown below, this error is larger than the accuracy of the mean profile. One could devise a method to first remove the unknown bias from each profile before averaging. However, to achieve 1-mgal accuracy from 30 repeat profiles, the unknown bias must be accurate to 0.1 m; if only three repeat profiles are available, then the bias must be known to an accuracy of 0.01 m. Such high accuracies are difficult to achieve because the profiles have a wide variety of lengths and contain many irregular data gaps. We have found that differentiation is a simple and effective way to suppress the radial orbit before averaging the repeat profiles. Moreover, once the *average vertical* deflection profile is computed, it can be integrated back to form an average height profile with an unknown bias.

### *Averaging Repeat Cycles*

After editing, applying the corrections, and differentiating the profiles, all 44 repeat cycles (~61 million observations) were loaded into two compact files, one for the ascending profiles and the other for the descending profiles. Each file has 244 columns representing the 244 equator crossings of the 17-day repeat cycle and 7000 rows representing the possible number of twice-per-second samples in a complete ascending or descending arc. A third dimension was used to store the 44 repeat cycles. Preprocessed vertical deflection profiles were interpolated onto the uniform alongtrack bins and placed in the file. The data were sampled at a rate of approximately two points per second (one point per 3.37 km alongtrack) so that a linear interpolation scheme could be used after the data were low-pass filtered (16-km half-amplitude, cutoff wavelength). To avoid storing latitude and longitude information, simple formulas, based on a circular orbit about a rotating elliptical Earth, were used to map the record position into time and geodetic latitude and longitude; profiles were assumed to be collinear.

After all of the data were loaded into the two files, the vertical deflections were averaged (i.e., sum of available points/number of available points). To remove remaining outliers, individual points were compared with the average. The point having the largest deviation was temporarily removed from the set, and the average was recomputed. If this point deviated by more than 4 standard deviations from the new average, then it was edited. This editing cycle was repeated until either all points passed the test or less than four points remained. This editing removed an additional 1.1% of the data. We found this final editing step to be quite important, although it requires that all 44 unfiltered repeat cycles reside on computer disk simultaneously. In addition to averaging and editing all 44 profiles, we also averaged and edited the first year of data (cycles 1–22) independently from the second year of data (cycles 23–44). These single-year averages are used below to estimate the resolution capabilities of vertical deflection profiles derived from the Geosat ERM.

## COVERAGE AND ACCURACY OF THE MEAN PROFILE

The ground track of the average vertical deflection profile is shown in Figure 1. Except for a few small areas of permanent sea ice, marine coverage along this 17-day profile is complete between latitudes of ±72°. While the coverage is quite uniform, large diamond-shaped gaps (~60 km), interstitial to the ground tracks, still remain so that the two-dimensional gravity field of the oceans is poorly resolved. In comparison with the previous GEOS 3 and Seasat satellite altimeter missions, the Geosat ERM has acquired important new data in areas of seasonal ice cover. For example, coverage of the extreme southern ocean and Antarctic margins is especially good [*Sandwell and McAdoo*, 1988]. Most Arctic Ocean areas have good coverage as well.

While the coverage of the Geosat ERM profile appears quite uniform, there are large variations in the number of repeat cycles that were available when computing the 2-year average. To illustrate this, we computed the average of the number of cycles available in 1° Mercator cells; both ascending and descending profiles were used to determine this average. When a profile intersected a 1° cell, the number of repeat cycles available was counted. This number (0–44) was averaged with all of the other points in that cell to determine the average number of repeat cycles in the cell. Since not every 1° cell is intersected by either an ascending or descending Geosat profile, the average number of repeat cycles was interpolated into the empty cells using a Gaussian weighting of surrounding cells containing data. As a global average, 29.7 profiles were used to form the mean profile (dark gray in Figure 2). For latitudes less than about 60°, bands of lower repeat-cycle

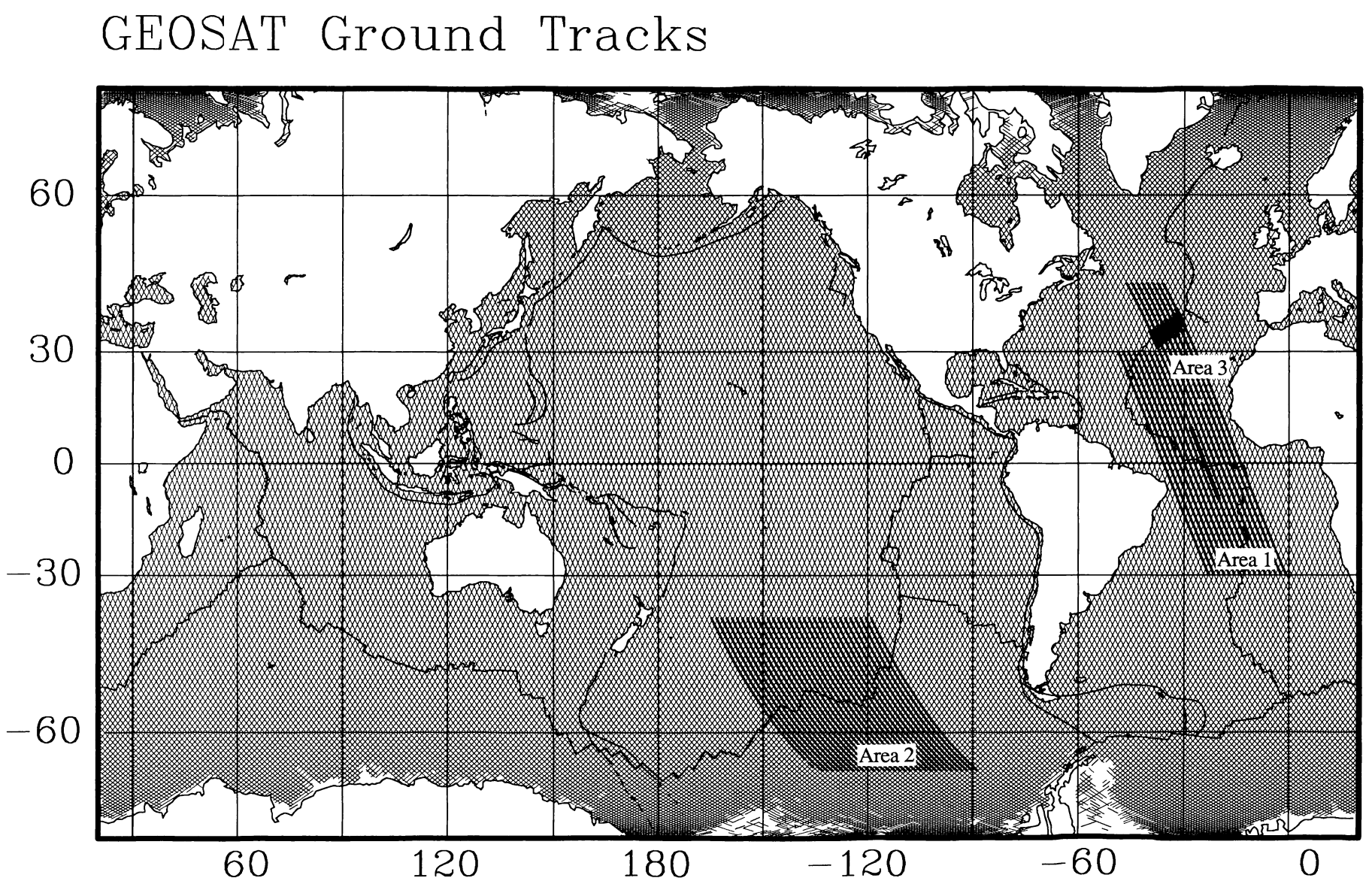


Fig. 1. Ground track of vertical deflection profile derived from 2 years of Geosat ERM data. Marine coverage is complete between ±72° except for a few small areas of permanent ice cover. Repeat profiles from areas 1, 2, and 3 were analyzed to estimate the accuracy and resolution of the 2-year average profile.

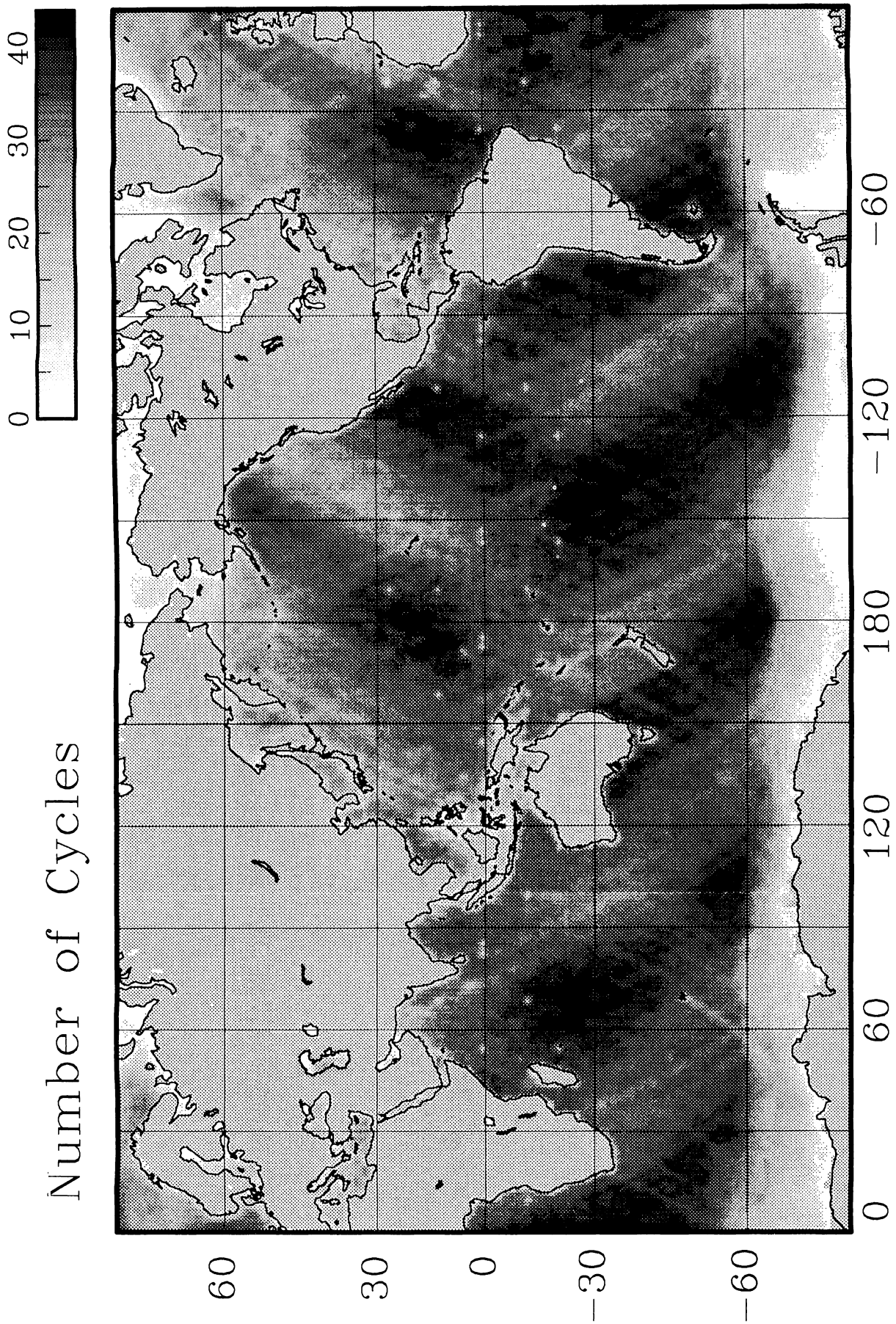


Fig. 2. Number of repeat cycles available when computing the 2-year average vertical deflection profile (0, white, 44, black). On average, 30 cycles were available out of a total of 44 cycles. Fewer cycles are available at high latitudes because of sea ice.

density reflect outages of altimeter data caused by oscillations in the pointing direction of the satellite away from nadir. At higher latitudes, low repeat cycle density (< 10) reflects the inability of the radar altimeter to gather data during times when the ocean is covered by ice. In some Arctic and Antarctic waters, where the repeat cycle density is less than about 5, the mean profile appears noisier, and as will be shown, it is significantly less accurate.

An example of vertical deflections derived from 44 repeat cycles crossing the equatorial Atlantic, is shown in Figure 3. This ascending track between latitudes of ±10° passes over the mid-Atlantic ridge and crosses two major-offset oceanic transform faults (see thickest line in Figure 1, area 1). The 44 individual repeat profiles show large-amplitude gravity signals as well as short-wavelength noise. The altimeter noise is reduced significantly by averaging all of the repeat cycles together (see average profile in Figure 3). Assuming a Gaussian distribution for the errors of the individual repeat cycles, the uncertainty in the mean profile (Figure 3, bottom) was computed as the standard deviation about the mean profile divided by the square root of the number of cycles used to form the mean profile. The uncertainty in this mean profile is less than 1 μrad. However, this is an especially accurate profile because unlike most profiles, more than 40 repeat cycles are available. Moreover, the profile crosses an area of low "oceanographic noise."

To estimate the accuracy of the average vertical deflection profile on a global basis, we calculated the uncertainty, as described above, and averaged it into 1° Mercator cells. As was done when computing the average number of repeat cycles (Figure 2), both the ascending and the descending passes were used in the average; the same Gaussian interpolation scheme was used to fill the diamond-shaped gaps of the 17-day ground track. The results are displayed in Figure 4 as a gray-tone image. Areas where the uncertainty of the mean is less than 1 μrad are white, while areas where the uncertainty is greater than 5 μrad are black. Intermediate uncertainties are displayed in gray shades according to the scale shown above the image. The average uncertainty, over all areas where more than two repeat cycles were available, is 1.6 μrad. However, it is apparent from Figure 4 that over most areas, the uncertainty is less than 2 μrad. Moreover, between latitudes of ±30° the uncertainty is usually less than 1 μrad. Areas where the uncertainty exceeds 5 μrad are confined mainly to high latitudes (> 60°) where sea ice is a problem.

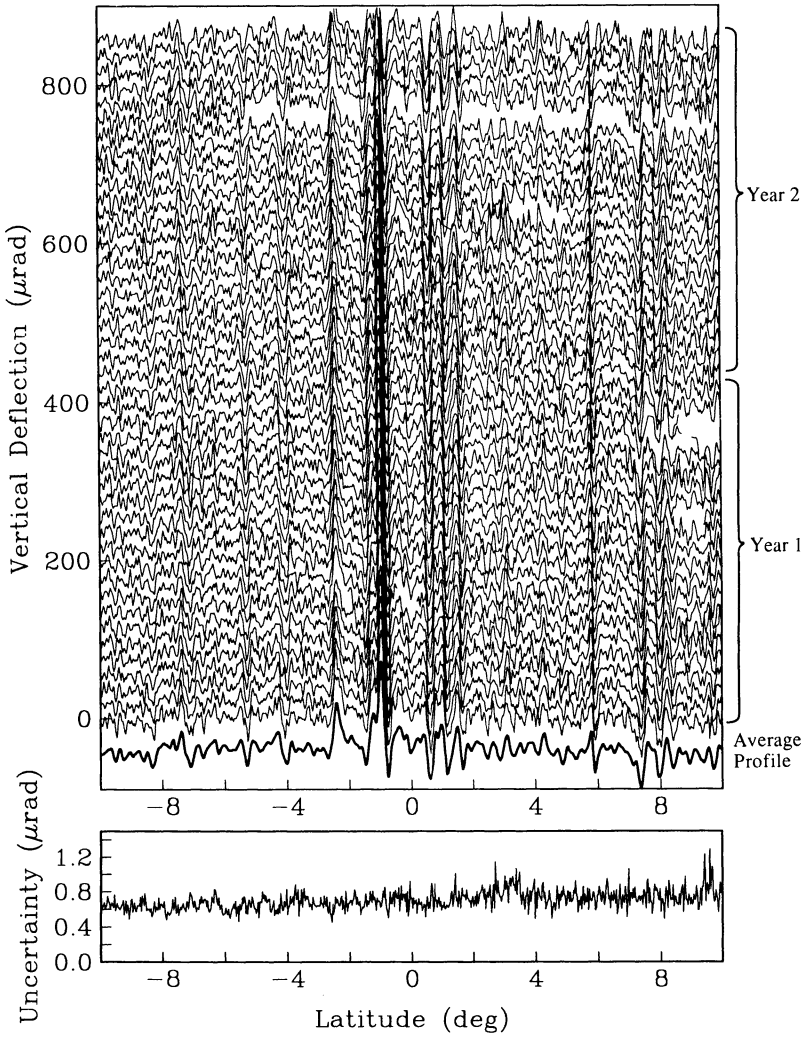


Fig. 3. (top) Example of 44 ascending vertical deflection profiles used to form the 2-year average profile. The ground track is shown as heaviest line in area 1, Figure 1. (bottom) The uncertainty of the average profile is the standard deviation of the individual profiles about the mean profile divided by the square root of the number of cycles. Uncertainties are less than 1 μrad (< 1 mgal) along this profile.

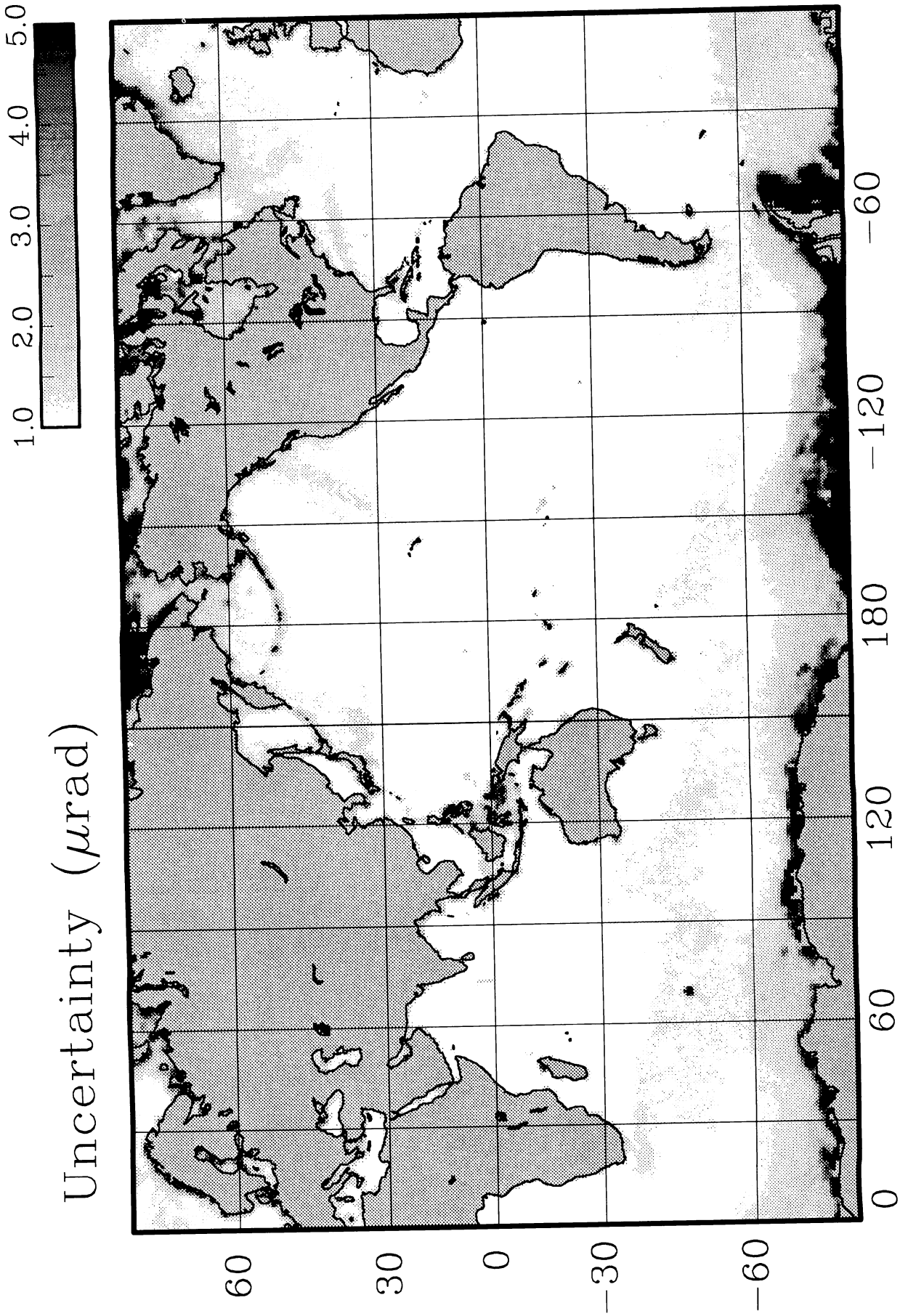


Fig. 4. Uncertainty in average vertical deflection profile (0 μrad, white, 5 μrad, black) was computed as the standard deviation about the average divided by the square root of the number of cycles. Uncertainties are less than 1 μrad at low latitudes (< 30°) and range from 2–5 μrad at higher latitudes.

The uncertainty of the mean profile depends on two factors. The most important factor is the number of cycles available to form the average. This can be seen from a comparison of Figures 2 and 4, where there is a strong negative correlation between the uncertainty and the number of cycles. Of course, the highest uncertainties occur in the areas with the lowest number of repeat cycles such as the areas of seasonal ice cover. In addition to the number of repeat cycles, the uncertainty also depends on the standard deviation or noise of the individual cycles. A gray-tone image of the standard deviation is shown in Figure 5. The standard deviation varies between about 4 and 8 μrad and has a global mean of 6.2 μrad. Several factors appear to influence the standard deviation of the individual repeat cycles. As will be shown below, the largest contribution to the standard deviation of the vertical deflection is short-wavelength (10- to 100-km wavelength) altimeter noise. The second largest contribution is the mesoscale variability of the oceans which tends to be composed of wavelengths greater than about 100 km [*Fu*, 1983; *Fu and Zlotnicki*, 1989] and is localized along western boundary currents and along the Antarctic Circumpolar Current [*Koblinsky*, 1988; *Sandwell and Zhang*, 1989]. At the high latitudes, radar reflections from errant icebergs may introduce considerable noise. These spurious radar reflections can be edited using the iterative method described above but only if more than three repeat cycles are available. For this reason, high standard deviation is also partially due to a low number of repeat cycles. Finally, many small areas of high standard deviation also occur near oceanic islands and coastlines; this could be due either to spurious radar reflections from land or short-wavelength tide model errors. It is interesting to note that the lowest standard deviations are sometimes associated with areas of shallow water such as Hudson Bay and the Falkland Plateau.

## RESOLUTION

### *Repeat Track Method*

We have used the repeat track method [*Brammer and Sailor*, 1980; *Marks and Sailor*, 1986; *LeSchack and Sailor*, 1988] to determine the resolution capabilities of Geosat ERM profiles. As outlined in these previous studies, sea surface height profiles consist of both geoid undulations ("signal") and "noise" (e.g., oceanographic variability, orbit error, measurement error, and errors in the ionospheric, atmospheric, and tidal corrections). Since geoid height is time invariant, repeating satellite altimeter profiles will measure a common geoid height signal. As in these previous studies, we assume that the nongeoidal part of the altimeter measurement varies with respect to time, so that a portion of this "noise" will be different from one repeat profile to the next. While oceanographic studies have shown that there is a permanent component of the sea surface topography associated with ocean circulation [*Levitus*, 1982], it has a relatively small amplitude (< 1 μrad) and consists primarily of long wavelengths (> 1000 km). In our resolution study we are interested in wavelengths less than 100 km, so permanent oceanography is not a problem.

As in the previous resolution studies, we examine the power spectra of the altimeter profiles, the power spectra of the difference between repeat profiles divided by $\sqrt{2}$ and finally, the spectral coherence between repeat profiles. The main difference between our analysis of Geosat ERM data and the previous analyses of Seasat and GEOS 3 data [*Marks and Sailor*, 1986] is that we analyze vertical deflection profiles instead of sea surface topography profiles. This difference changes the amplitude and shape of the power spectra, but as we show next, it has no effect on the coherence estimates.

Consider a sea surface topography profile $h(x)$, where $x$ is distance along the satellite track. To form vertical deflection $s(x)$, we take the derivative of $h(x)$ with respect to $x$,

$$s(x) = \frac{\partial h}{\partial x} \tag{1}$$

In the Fourier transform domain, the vertical deflection $S(k)$ and height $H(k)$ are related by

$$S(k) = 2\pi i k H(k) \tag{2}$$

where $k = 1/\lambda$ is the wave number, $\lambda$ is wavelength and $i = \sqrt{-1}$.

Therefore the power spectrum of the vertical deflection profile ($P_s = SS^*$, where $S^*$ is the complex conjugate of $S$) is related to the power spectrum of the height profile ($P_h = HH^*$) by

$$P_s(k) = (2\pi k)^2 P_h(k) \tag{3}$$

As is shown in this equation, the power spectrum of the vertical deflection profile falls off less rapidly with increasing wave number than does the power spectrum of the height profile. To relate the vertical deflection power spectrum to the height power spectrum, one simply divides by $(2\pi k)^2$.

The spectral coherence between two height profiles $h_1$ and $h_2$ is defined as

$$\rho(k) = \frac{|H_1 H_2^*|^2}{H_1 H_1^* H_2 H_2^*} \tag{4}$$

where $H_1 H_2^*$ is the cross spectrum of $h_1$ and $h_2$. To derive an expression for the spectral coherence between two vertical deflection profiles $s_1$ and $s_2$, one substitutes $S(k)/2\pi ik$ for $H(k)$ in equation (4). After cancelling terms in the numerator and denominator, it is clear that except at zero wave number, the coherence computed with height profiles is identical to the coherence computed with the vertical deflection profiles.

$$\rho(k) = \frac{|S_1 S_2^*|^2}{S_1 S_1^* S_2 S_2^*} \tag{5}$$

Therefore our analysis of Geosat vertical deflection profiles can be compared directly with the previous analyses of Seasat and GEOS 3 profiles. Geosat ERM profiles were selected from three areas for the resolution analysis.

### *Area 1: High Signal and Low Noise*

The objective of our first analysis was to estimate the signal, noise, and resolution capabilities of unaveraged and averaged Geosat repeat profiles. For this analysis, 16 ascending profiles crossing the equatorial Atlantic were analyzed (Area 1 in Figure 1). This area was selected because nearly all of the ascending repeat cycles are available (Figure 2) and the standard deviations of the cycles is relatively low (Figure 5). In addition, this is an area where the vertical deflection signals are quite large (Figure 3). Because the signal is high and the noise is low we expect the resolution estimates from this area to be representative of the best that can be done with Geosat ERM data.

The first experiment used unaveraged Geosat profiles. Data from repeat cycles 3 and 25 were extracted from the large ascending stack file such that corresponding points were always available. This guaranteed that that the profiles were aligned properly and that any small data gaps were common to both data sets. Each of the 16 profiles was truncated to a length of 2048 points for the

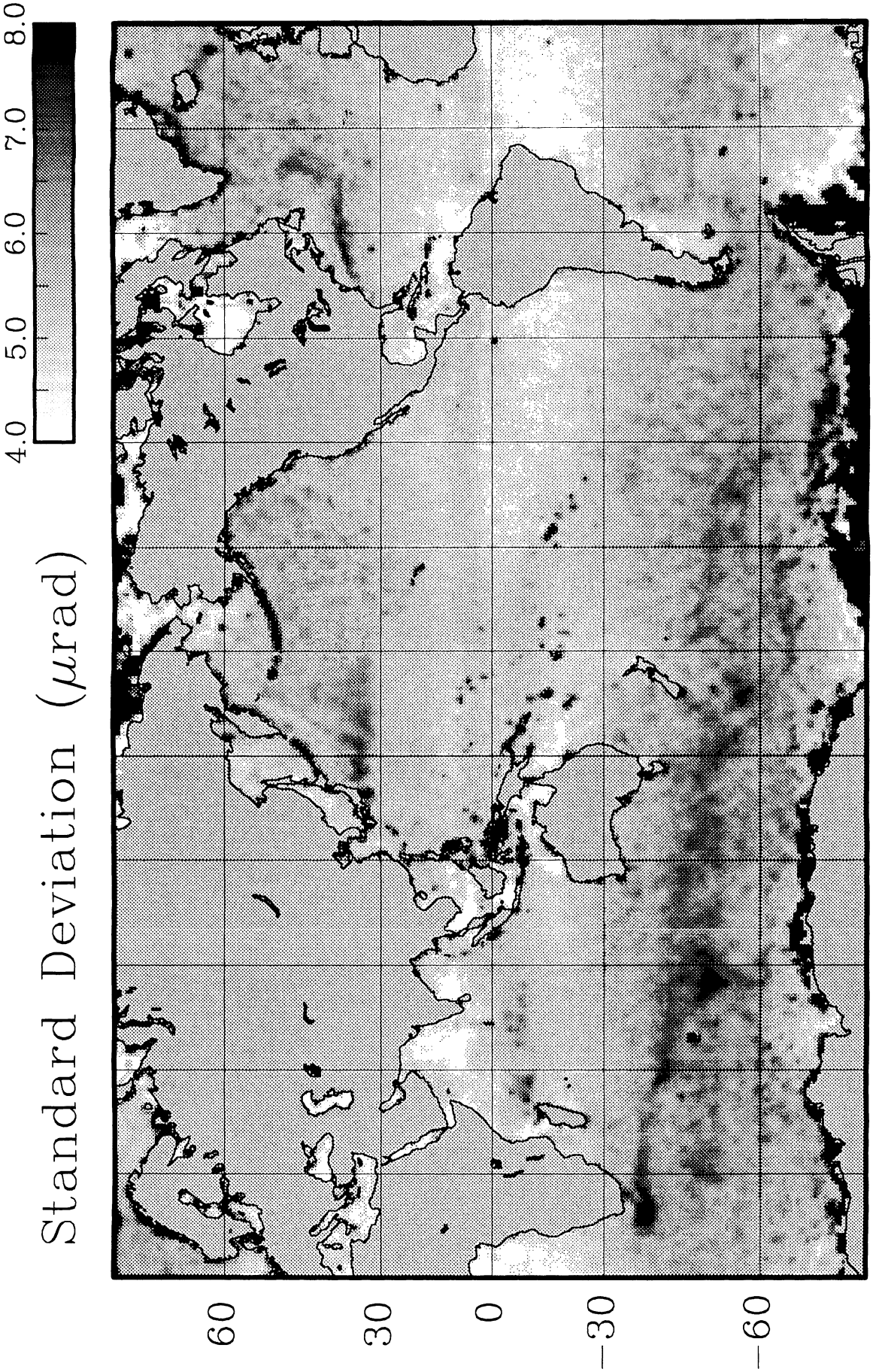


Fig. 5. Standard deviation of individual vertical deflection profiles about the mean profile (4 μrad, white, 8 μrad, black). Standard deviations reflect uniform short-wavelength altimeter noise as well as spatially variable mesoscale oceanography. High standard deviations in Arctic and Antarctic areas are caused by poor coverage due to sea ice.

spectral analyses. The Welch method of power and cross-spectral estimation [*Oppenheim and Schafer*, 1975] was applied to the profiles using the Matlab signal processing library [*Little*, 1986]. To obtain reliable spectral estimates, each of the 16 profiles was subdivided to form 32 segments of 1024 points. Each segment was detrended and windowed with a Hanning function before calculation of the discrete Fourier transform. Finally, power spectra and cross spectra from each of the 32 transforms were added together.

The resolution capabilities of single (unaveraged) Geosat profiles are shown in Figure 6. The horizontal axis is wave number $k$ or inverse wavelength. Wavelengths range from 1740 km to 10 km. The shortest wavelength resolvable is 6.6 km (one point per 0.49 s). The power spectral density (PSD) of cycle 3 (data PSD) and the PSD of the difference between cycle 3 and cycle 25 divided by $\sqrt{2}$ (noise PSD), are shown in Figure 6*a*. The absolute values of the power spectra have little meaning because they depend on how the data were segmented, detrended, and windowed. As is typical for marine gravity power spectra, the data PSD shows a general decrease in power with increasing wave number.

In contrast to the data PSD, the noise PSD initially increases with increasing wave number and then flattens and finally decreases. The initial increase is caused by taking the derivative of white noise, and thus it has a slope of about $k^2$. The flattening and final decrease in the noise PSD are due partially to the low-pass Gaussian filter that was applied to the profiles before they were interpolated. However, the noise PSD decreases much more rapidly than could be caused by the Gaussian interpolation. Thus this spectral characteristic is inherent in the raw data; a similar behavior is shown by *LeSchack and Sailor* [1988]. For these unaveraged profiles, the data PSD and the noise PSD merge at a wavelength of about 25 km (Figure 6*a*).

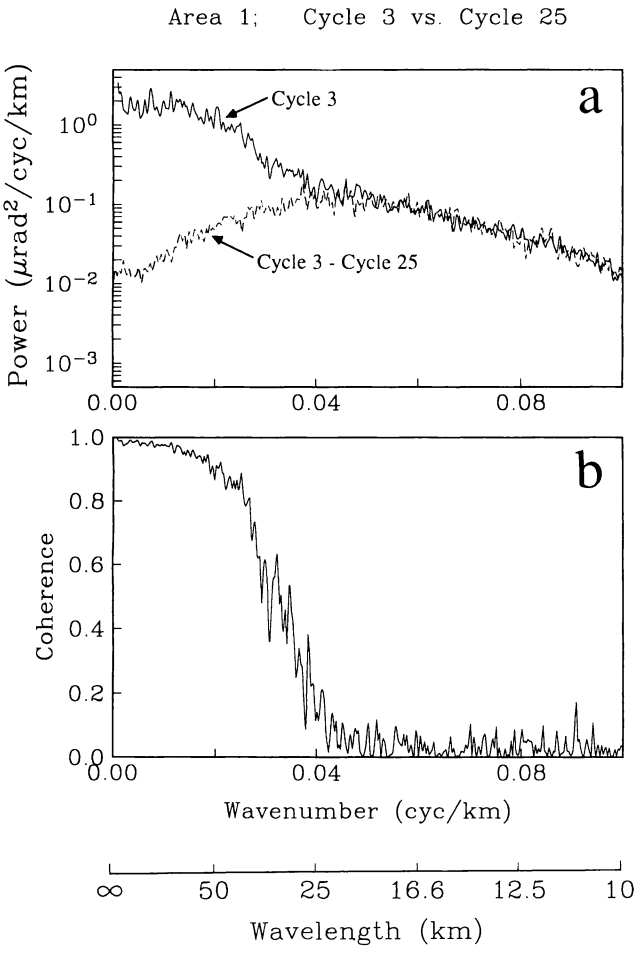


Fig. 6. (*a*) Power spectral density versus wave number (1/wavelength) for 16 ascending profiles (area 1, Figure 1) from repeat cycle 3 (solid curve). The dashed curve shows PSD of cycle 3 through cycle 25 divided by $\sqrt{2}$. The data PSD and the noise PSD merge at a wavelength of 24.7 km for these unaveraged Geosat profiles. (*b*) Coherence between cycle 3 and cycle 25 (1, coherent; 0, incoherent). Coherence falls to 0.5 at a wavelength of 31.3 km. This resolution is typical of individual Geosat profiles.

The coherence between cycles 3 and 25 is shown in Figure 6*b*. As can be seen in equation (5), the coherence is equal to 1 when two series are correlated and is equal to 0 when two series are uncorrelated. A conservative estimate of the resolution capability of repeat profiles is the point where the coherence falls to 0.5. For these unaveraged profiles this 0.5 coherence occurs at a wavelength of 31.3 km. The coherence falls to 0.1 at a wavelength of 24.7 km, which also roughly corresponds the point where the data PSD and the noise PSD merge (Figure 6*a*). These resolution estimates are summarized in Table 1 along with the rms deviation of cycle 3 (rms signal of 16.5 μrad), the rms difference between cycle 3 and cycle 25 divided by $\sqrt{2}$ (rms noise of 4.7 μrad), and the average difference between cycle and cycle 25 (-0.04 μrad). The average difference between repeat profiles reflects the absolute repeatability of the data. In all cases it is less than 0.1 μrad.

To illustrate how the noise is reduced and resolution is increased by averaging many repeat cycles, we compared the average vertical deflection profile for the first year of the Exact Repeat Mission to the average profile for the second year. The 1-year average data from area 1 were processed in exactly the same way as the data from cycle 3 versus cycle 25 were processed. Averaging many repeat cycles reduces the rms noise from 4.7 μrad to 1.06 μrad. Since only a maximum of 22 repeat cycles were used in the 1-year averages, the noise was not reduced to the submicroradian levels seen in Figure 4. The PSD and coherence for year 1 versus year 2 are shown in Figure 7. In comparison with the unaveraged profiles (Figure 6), the year 1 versus year 2 noise PSD is significantly lower at all wavelengths; the data PSDs are similar at wavelengths greater than 30 km. The reduction in the noise PSD causes the two PSDs to merge at a shorter wavelength (13.7 km instead of 24.7 km). As expected, the wavelength where the coherence falls to 0.5 also decreases from 31.3 km to 19.4 km. Therefore averaging many repeat cycles reduces the noise level, which in turn increases the resolution of the data.

### *Area 2: Low Signal and High Noise*

To estimate the resolution of averaged Geosat repeat profiles for the case where the signal is relatively low and the noise is relatively high, we chose 32 ascending profiles in the extreme South Pacific that cross the Antarctic Circumpolar Current (ACC) (Figure 1, area 2). The vertical deflection signal is relatively low (rms of 9.3 μrad) in this area because there are fewer fracture zones and the seafloor in this area is smooth compared with the equatorial Atlantic (area 1, rms of 15.8 μrad). The noise is relatively high for this area (rms of 1.57 μrad versus 1.06 μrad for area 1) because some repeat cycles are missing (Figure 2) and the standard deviation of the individual cycles is greater (Figure 5). As shown next, and in previous studies [e.g., *Cheney et al.*, 1983], the higher noise level in this area can be attributed to mesoscale (100 km to 1000 km) variations in sea surface slope associated with the ACC.

For this experiment the average of the first year of repeat cycles (year 1) was compared with the average of the second year (year

TABLE 1. Summary of Resolution Estimates

| Area | Comparison | Signal, rms μrad | Noise, rms μrad | Mean Difference, μrad | Resolution (ρ = 0.5), km | Resolution (ρ = 0.1), km |
|---|---|---|---|---|---|---|
| 1 | Cycle 3 versus 25 | 16.45 | 4.68 | -0.04 | 31.3 | 24.7 |
| 1 | Year 1 versus 2 | 15.82 | 1.06 | 0.03 | 19.4 | 13.7 |
| 2 | Year 1 versus 2 | 9.33 | 1.56 | 0.03 | 26.3 | 20.0 |
| 3 | Year 1 versus 2 | 17.29 | 1.33 | 0.05 | 22.2 | 18.2 |
| Mid-Atlantic | Year 1 versus 2 | 20.93 | 1.20 | 0.04 | 17.2 | 14.3 |

2). Each of the 32 profiles was detrended, windowed, and Fourier transformed as in the previous cases. In comparison with area 1 (Figure 7), the data PSD for this area 2 (year 1 in Figure 8*a*) is lower for wavelengths greater than 20 km and higher at shorter wavelengths. The area 2 noise PSD (year 1 versus year 2) is consistently higher at all wavelengths than the corresponding noise PSD for area 1. In addition, there is a prominent peak in the area 2 noise PSD for wavelengths greater than 100 km (stippled area in Figure 8*a*). We believe that this noise peak is due to changes in ocean currents causing differences in sea surface slope between year 1 and year 2. The relatively high noise in area 2, along with the relatively low signal, causes the data PSD and the noise PDS to merge at a wavelength of 20 km.

The coherence (Figure 8*b*) reflects this lower signal-to-noise ratio and falls to a value of 0.5 at a wavelength of 26.3 km; the 0.1 coherence again occurs at the point where the signal and noise PSD merge (20 km). Therefore the lower signal-to-noise ratio for area 2 relative to area 1 results in poorer resolution (26.3 km versus 19.4 km). It is interesting to note that the noise due to the mesoscale ocean variability does not influence the short-wavelength resolution capabilities of these satellite altimeter profiles. The limiting factors are poorly understood short-wavelength "measurement noise" and the number of repeat cycles available in the average. The overall accuracy of the average vertical deflection profile is, however, limited by basin scale and mesoscale oceanography.

*Area 3: Validation*

To determine if our averaged vertical deflection profiles and coherences depend on editing criteria, interpolation algorithm, or

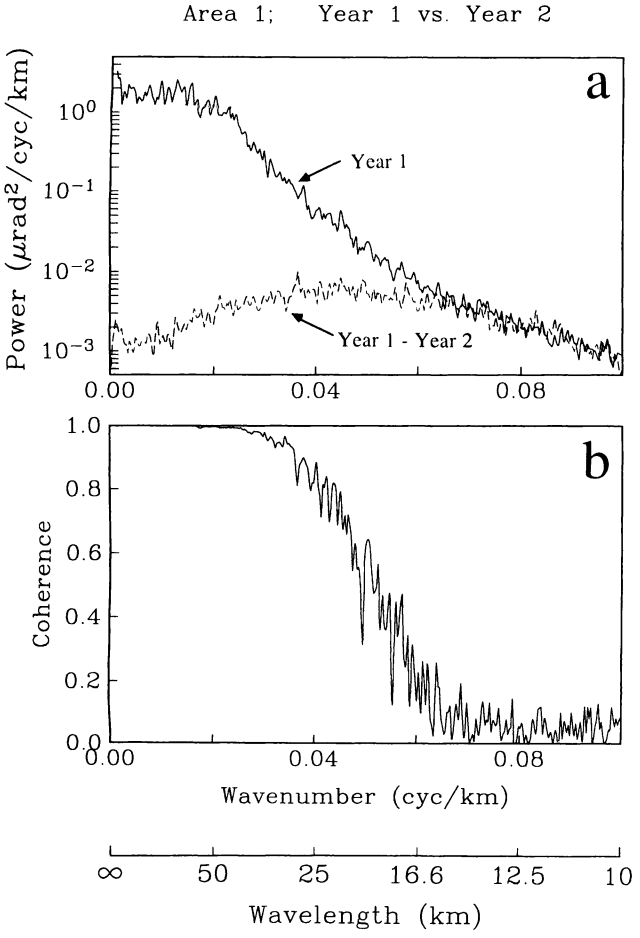


Fig. 7. (*a*) PSD of the average repeat of cycles 1–22 (year 1) and the PSD of the difference between the year 1 and year 2 averages divided by $\sqrt{2}$. Averaging reduces the noise so that the two PSDs merge at 13.7 km instead of 24.7 km for unaveraged data. (*b*) Coherence falls to a value of 0.5 at a wavelength of 19.4 km in contrast to 31.3 km for the unaveraged data (see Figure 6).

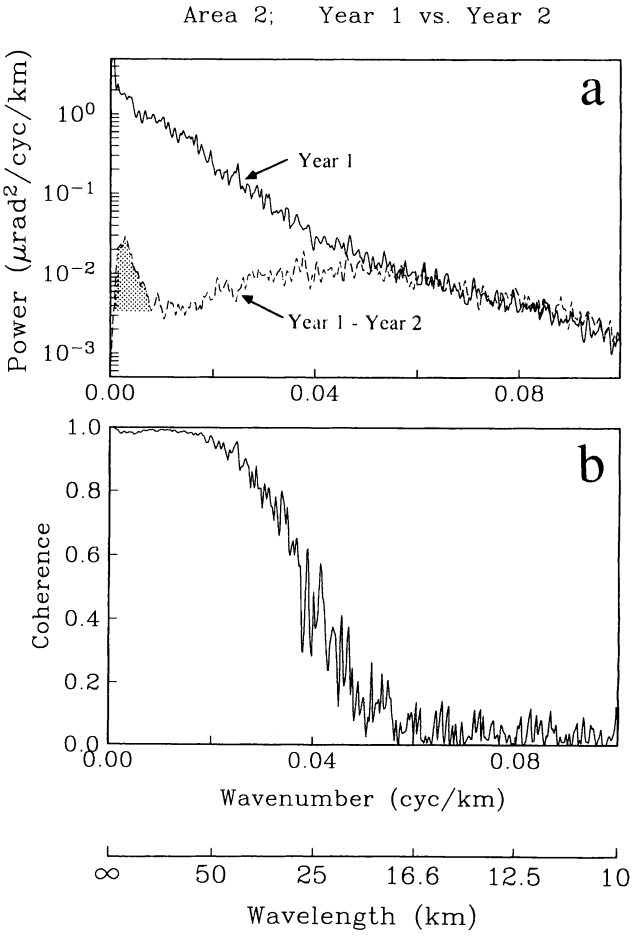


Fig. 8. (*a*) Data PSD (year 1) and noise PSD (year 1 versus year 2) for 32 ascending profiles from area 2, Figure 1. Area 2 has lower signal and higher noise than area 1. The stippled area in noise PSD reflects oceanograph noise of the Antarctic Circumpolar Current. (*b*) Coherence falls to 0.5 at a wavelength of 26.3 km, poorer resolution than area 1 (19.4 km).

the spectral analysis method, we conducted a fully independent analysis of eight profiles which comprise area 3 (Figure 1). Each of these eight profiles is 2900 km long, and each crosses the mid-Atlantic Ridge. The solid curve in Figure 9*b* shows the coherences recovered from these eight profiles using all of the procedures described above. The dashed lines, however, depict coherences that were derived independently (i.e., different investigators, different algorithms, different computers). First, preprocessing procedures were different. Data editing was slightly less stringent. Heights were compressed from 10 per second to 2 per second using a sliding quadratic over 2-s intervals. The resulting 2-per-second data were interpolated into uniform alongtrack bins using a cubic spline; no Gaussian low-pass filter was applied. Finally, a slightly different technique was used to perform the spectral analysis. The basic algorithm was the same (i.e., Welch's modified averaged periodogram) but the segmenting and windowing were different. Eight profiles were placed in tandem, padded with zeros to obtain input sequences of 8192, segmented into 64 subsequences of 128 points, windowed with a Parzen window, and then subjected to spectral analysis. The resulting dashed curve (long dashes) in Figure 9*b* agrees well with the independently estimated solid curve. This validation suggests that the whole procedure of forming vertical deflection profiles, averaging them together, and analyzing them is relatively insensitive to the criterion or algorithms employed. We shall use this alternate approach to analyze short segments of these eight profiles in the vicinity of the mid-Atlantic Ridge.

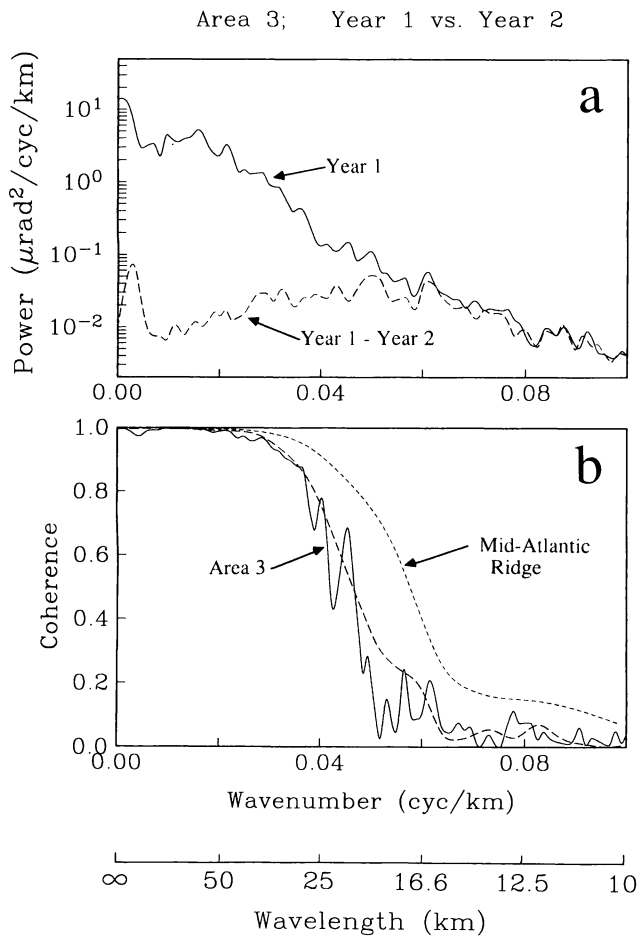


Fig. 9. (*a*) Data PSD (year 1) and noise PSD (year 1 versus year 2) for eight ascending profiles from area 3, Figure 1 (latitude range 20°–45°). (*b*) Coherence as shown by the solid curve was calculated as in other examples; coherence shown by the long-dashed curve was calculated by an independent investigator using independent data editing, independent data averaging, and independent spectral analysis. Thus results do not depend on investigator or methods used. Coherence as shown by the short-dashed curve is for eight short profiles spanning shallow water of the mid-Atlantic ridge. Generally, higher coherence reflects higher gravity signal and less upward continuation in shallow water.

*Area 3': High Signal, Low Noise, and Shallow Water*

As a final experiment we selected eight short profiles (128 points) that focus in the mid-Atlantic ridge axis. These eight profiles are a subset of the eight long profiles of area 3 (heavy lines in area 3, Figure 1). This area is characterized by low noise and very high amplitude (20.9 μrad rms), short-wavelength vertical deflection signals. In addition, the seafloor in this area is relatively shallow (< 3 km). Because of upward continuation from the seafloor (depth $z$), the amplitude of the vertical deflection measured at the sea surface is attenuated by a factor of $\exp(-2\pi kz)$ with respect to the amplitude of the vertical deflection measured on the seafloor. For example, anomalies having wavelengths of 20 km are attenuated by a factor of 0.39 in a 3-km-deep ocean and by 0.18 in a 5.5-km-deep ocean. The objective of this final experiment was to estimate the best resolution that is available over individual, shallow geologic structures.

The results of the coherence between year 1 averages and year 2 averages are shown in Figure 9*b* (short-dashed curve). Because these eight profiles were only 128 points long, they were further subdivided by 4 to increase the reliability of the coherence estimates. The coherence falls to 0.5 at a wavelength of 17.2 km. Although the coherence does not fall to 0.1 because there were not enough data points in the analysis, one would estimate that the 0.1 coherence occurs at a wavelength of 14.3 km. The results of this final analysis suggest that over individual geologic structures in shallow water, averaged vertical deflection profiles from Geosat ERM can resolve features having wavelengths of about 16 km. This corresponds to a half-wavelength resolution of only 8 km!

## CONCLUSIONS

We find that averaging vertical deflection profiles along repeat ground tracks significantly improves the coverage, accuracy, and resolution of satellite altimeter data. Improvements in coverage occur in Arctic and Antarctic areas where seasonal ice interferes with the altimeter measurements. Improvements in accuracy depend mainly on the number of repeat cycles that are averaged together. The standard deviation of individual vertical deflection profiles (before averaging) suggests that they are accurate to about 6 μrad. After averaging one year of data (~15 repeat cycles) the differences between the year 1 average and the year 2 average indicate that the accuracy has improved by the square root of the number of cycles in the average from 6 μrad to 1-2 μrad. Using this random noise model, we estimate that the 2-year average profile is accurate to less than 1 μrad at lower latitudes (< 30°) and is accurate to 2–5 μrad at higher latitudes.

Since the power in the vertical deflection profiles decreases rapidly with decreasing wavelength, improvements in accuracy (i.e., reduction in noise) lead to improvements in resolution as well. Figure 10 illustrates the improvements in resolution that have occurred since the GEOS 3 mission where we have plotted coherence between repeat profiles from GEOS 3, Seasat, Geosat ERM, and 1-year-average Geosat ERM. The GEOS 3 and Seasat results were taken from *Marks and Sailor* [1986] while the Geosat and Geosat stack results are smoothed coherences from Figures 6 and

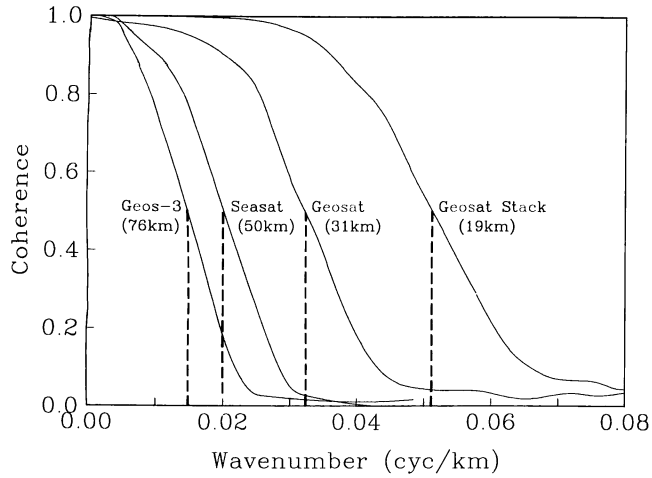


Fig. 10. Comparison of smoothed coherences between repeat GEOS 3, Seasat, Geosat, and stacked Geosat profiles. GEOS 3 and Seasat results are from *Marks and Sailor* [1986]. Improvements in resolution from 76 km for GEOS 3 to 31 km for Geosat reflect improvements in altimeter design. The improved resolution of the stacked Geosat data is due to averaging 22 repeat cycles.

7 of our study. Improvements in altimeter design have resulted in resolution improvements from 76 km for GEOS 3 to 50 km for Seasat to 31 km for Geosat. An additional resolution improvement to 19 km was achieved by averaging 1 year of Geosat ERM profiles; we expect the 2-year average to have only slightly better resolution than the 1-year average. It should be pointed out that all of these resolution estimates are based on a somewhat conservative definition of resolution limit (i.e., coherence of 0.5). Moreover, in geophysical investigations of individual features having large amplitudes (e.g., mid-Atlantic ridge), shorter-wavelength signals can be observed. Nevertheless, it is useful to have a well-defined and consistent measure of the resolution capabilities of these instruments.

Our results indicate that complete two-dimensional coverage of the marine gravity field is possible with a long-lifetime satellite altimeter mission. For example, to obtain a global marine gravity field with an accuracy of 2 μrad (2 mgal) and a 24-km wavelength resolution requires a 4.5-year altimeter mission. It takes 180 days to attain a ground track having a cross-track resolution of 16-km wavelength at the equator and better resolution at higher latitudes. Nine of these half-year cycles would reduce the random noise from 6 μrad to 2 μrad. We find that the less accurate Geosat ERM orbits are sufficient to obtain a marine gravity field with high accuracy and high resolution. Moreover, the corrections supplied with the GDRs are not the main factor limiting the accuracy of the gravity field. The reason that the orbits and corrections are accurate enough is that they are long-wavelength errors that are suppressed by differentiation. Thus a relatively inexpensive, relatively low accuracy, long-lifetime satellite altimeter mission could completely map the marine gravity field with a high accuracy and resolution. Such a data set would certainly revolutionize our understanding of marine geology and geophysics.

As a final note, the 2-year average vertical deflection profile presented here will be placed in the National Geophysical Data Center, Boulder, Colorado, for others to use and evaluate. The data file consists of time, latitude, longitude, geoid height, vertical deflection (2-year average), and the uncertainty of the vertical deflection profile. The average geoid height profile is formed by integrating continuous segments of vertical deflection profiles and fitting the average height profile to the spherical harmonic surface defined by the PGS-3337 geoid model to degree and order 40 [*Marsh et al.*, 1989].

*Acknowledgments.* We thank Russell Agreen, Nancy Doyle, Robert Cheney, Lawrence Miller and Bruce Douglas for their rapid and accurate processing of the Geosat Geophysical Data Records. This work was supported by the NASA Geodynamics Program (NAG 1266) and the National Geodetic Survey.

## REFERENCES

Born, G. H., J. L. Mitchell, and G. A. Heyler, Design of the Geosat exact repeat mission, *Johns Hopkins APL Tech. Dig., 8*, 260–266, 1987.

Brammer, R. F., Estimation of the ocean geoid near the Blake Escarpment using GEOS 3 satellite altimetry data, *J. Geophys. Res., 84*, 3843–3851, 1979.

Brammer, R. F., and R. V. Sailor, Preliminary estimates of the resolution capability of the Seasat radar altimeter, *Geophys. Res. Lett., 7*, 193–196, 1980.

Cheney, R. E., J. G. Marsh, and B. D. Beckley, Global mesoscale variability from collinear tracks of Seasat altimeter data, *J. Geophys. Res., 88*, 4343–4354, 1983.

Cheney, R. E., B. C. Douglas, R. W. Agreen, L. Miller, and D. L. Porter, Geosat altimeter geophysical data record (GDR) user handbook, *NOAA Tech. Memo. NOS NGS-46*, 32 pp., Natl. Ocean Serv., Rockville, Md., 1987.

Fu, L.-L., On the wave number spectrum of oceanic mesoscale variability observed by the Seasat altimeter, *J. Geophys. Res., 88*, 4331–4341, 1983.

Fu, L.-L. and V. Zlotnicki, Observing oceanic mesoscale eddies from Geosat altimetry: Preliminary results, *Geophys. Res. Lett., 16*, 457–460, 1989.

Koblinsky, C., Geosat vs. Seasat, *Eos Trans AGU, 69*, 1026, 1988.

LeSchack, A. R., and R. V. Sailor, A preliminary model for Geosat altimeter data errors, *Geophys. Res. Lett., 15*, 1203–1206, 1988.

Levitus, S., Climatological atlas of the world ocean, *NOAA Prof. Pap. 13*, U.S. Dept. of Commer., Rockville, Md., 1982.

Little, J. N., *MATLAB Signal Processing Toolbox*, The Math Works, South Natick, Mass., 1986.

Marks, K. M., and R. V. Sailor, Comparison of GEOS 3 and Seasat altimeter resolution capabilities, *Geophys. Res. Lett., 13*, 697–700, 1986.

Marsh, J. G., and T. V. Martin, The Seasat altimeter mean sea surface model, *J. Geophys. Res., 87*, 3269–3280, 1982.

Marsh, J. G., C. J. Koblinsky, F. Lerch, S. M. Klosko, J. W. Robbins, R. G. Williamson, and G. B. Patel, Dynamic sea surface topography, gravity, and improved orbit accuracies from the direct evaluation of Seasat altimeter data, *J. Geophys. Res.*, in press, 1989.

Oppenheim, A. V., and R. W. Schafer, *Digital Signal Processing*, 566 pp., Prentice-Hall, Englewood Cliffs, N.J., 1975.

Sailor, R. V., Determination of the resolution capabilities of the Seasat radar altimeter, observations of the geoid spectrum, and detection of seamounts, *Rep. TR-3751*, The Analytic Sciences Corp., Reading, Mass., 1982.

Sailor, R. V., and A. R. LeSchack, Preliminary determination of the Geosat radar altimeter noise spectrum, *Johns Hopkins APL Tech. Dig., 8*, 182–183, 1987.

Sandwell, D. T., and D. C. McAdoo, Marine gravity of the southern ocean and Antarctic margin from Geosat, *J. Geophys. Res., 93*, 10,389–10,396, 1988.

Sandwell, D. T., and B. Zhang, Global mesoscale variability from the Geosat Exact Repeat Missions: Correlation with ocean depth, *J. Geophys. Res., 94*, 17;,971–17,984, 1989.

Zlotnicki, V., L.-L. Fu, and W. Patzert, Seasonal variability in global sea level observed with Geosat altimetry, *J. Geophys. Res., 94*, 17,959–17,969, 1989.

D. C. McAdoo, National Geodetic Survey, Charting and Geodetic Services, National Ocean Service, NOAA, Rockville, MD 20852.

D. T. Sandwell, Geological Research Division, Scripps Institution of Oceanography, La Jolla, CA 92093.

(Received July 25, 1989;
accepted September 20, 1989.)